

RADAR CALIBRATION USING POLARIMETRIC OBSERVATIONS WITH RAIN ATTENUATION CORRECTION

Ahoru Adachi*, Takahisa Kobayashi, Hiroshi Yamauchi and Shigeru Onogi
Meteorological Research Institute, Tsukuba, Japan

1. INTRODUCTION

The accuracy of radar-based rainfall rate is limited by the calibration of radar reflectivity Z_H , which must be measured within 1 dB for rainfall estimates to have an accuracy of 15 %. Studies (e.g. Goddard et al. 1994) have shown that calibration of Z_H can be achieved within 1 dBZ using the relationship between Z_H , differential reflectivity (Z_{DR}), and specific differential propagation phase (K_{DP}). However, since this method does not take the rain attenuation effect into account, it is not easy for C-band radar to get higher accuracy with this method and is impractical for X-band radar to use (Gourley et al. 2009). In this study, we propose a calibration algorithm immune to rain attenuation. In the algorithm, DSD parameters and rainfall rate were retrieved as a part of rain attenuation correction, which was evaluated by comparisons with disdrometer measurements on the ground.

2. INSTRUMENTATION AND DATA RETRIEVAL TECHNIQUES

The data obtained by the Meteorological Research Institute (MRI) advanced C-band solid-state polarimetric radar (MACS-POL radar, Yamauchi et al. 2012) were used in the present study. The radar is equipped with solid-state amplifiers, and the transmitted pulses have widths of 1 μ s and 129 μ s alternatively, a beam width of 1°, a frequency of 5.37 GHz, a peak power of 4 kW with a pulse compression technique (Anraku et al. 2013). Prior to calibrating Z_H , we have checked the quality of the raw polarimetric quantities including vertical measurements for calibrating Z_{DR} . The specific attenuation, A_H and specific differential attenuation A_{DP} were estimated from observed Z_H and Z_{DR} by use of a polarimetric radar simulator (Kobayashi et al. 2012), and attenuation corrections were applied for the Z_H and Z_{DR} measurements to calculate theoretical K_{DP} , which is then integrated in the radial direction to yield a theoretical differential propagation phase (Φ_{DP}). The backscatter differential phase (δ_{co}) is not considered in the algorithm.

Differences between theoretical and observed Φ_{DP} at the end of rain path ($\Delta\Phi_{DP}$) are attributable to the bias in Z_H measurements. The observed Φ_{DP} is not input into the attenuation correction algorithm but used as a reference. Also note that this method does not need to DSD measurements on the ground for reference. This method provides absolute calibration of Z_H when the radome is dry. In addition, this method can estimate the bias in Z_H due to the wet radome when it rains at the radar site (Bringi et al. 2006).

3. SIMULATION AND COMPARISON CONDITIONS

Raindrop spectra were modeled with a normalized gamma distribution (Bringi and Chandrasekar 2001) assuming a shape parameter (μ) setting of 5, with raindrop shapes being represented by the Brandes et al. (2002, 2005) model for equivalent volumetric diameter, $De \leq 8$ mm, but the axis ratio is set to unity for $De < 0.5$ mm. Temperature of raindrops needed to calculate complex refraction index was estimated from surface temperature and set to 20° C for the case on 7 July (Fig. 1) and 10° C for the rest. Rainfall rates were estimated from DSD parameters including N_w and D_0 derived from the proposed algorithm and terminal fall velocities V_T by Lhermitte (1990). The reliability of the method was confirmed by comparing the estimated rainfall rate from the radar at 1.0° elevation angle with that estimated from DSD derived from an optical disdrometer (Parsivel) on the ground at Sekiyado (SYD) located about 32 km apart from the radar (Fig. 2). The difference in observational times arisen from height difference (the radar beam center observed precipitation about 670 m above the Sekiyado station) was ignored in the comparisons. As the rainfall rate based on the DSD obtained by a Parsivel has been reported to have an overestimation tendency when the rainfall rate was high (e.g. Thurai et al. 2011; Tokay et al. 2013), we recalculated DSD to obtain rainfall rate based on Adachi et al. (2013) before the comparisons. Time resolutions are about 4 min. for the radar and 1 min. for the disdrometer measurements, respectively.

* Corresponding author address: Ahoru Adachi, MRI, Dept. of Observation System, Tsukuba 305-0052, Japan; email: aadachi (at) mri-jma.go.jp

4. RESULTS

4.1 Weak Rain

Range profiles of raw observed Φ_{DP} and smoothed-observed Φ_{DP} for the 30° azimuth valid at 0253 JST 07 July 2010 appear in Fig. 1. Rainfall rate in this direction was not very strong, which was supported by a gradual increase of Φ_{DP} with range. Weak rain region was chosen to suppress effects of the rain attenuation along the radial. The first 38 km of the data were contaminated by clutters in no rain region suggesting the radome was dry; beyond that distance attenuation-corrected theoretical Φ_{DP} progresses along with observed Φ_{DP} up to 90 km. After this range, observed Φ_{DP} begins to decrease because of local mixture of ice particles which is supported by low ρ_{HV} (not shown). The red curve shows theoretical Φ_{DP} without rain attenuation correction. The difference of the two theoretical Φ_{DP} profiles shows calibration of Z_H may have a bias of 0.7 dB if effects of rain attenuation are not considered even in weak rain at C-band, which is consistent with the results of Gourley et al. (2009).

4.2 Heavy Rain

We applied the proposed algorithm for a heavy rain region, in which effects of rain attenuation is expected quite large. The radar reflectivity field observed by the MACS-POL radar at 07:54 JST on 3 December 2010 indicates a heavy convective rain line approaching toward the MRI site from west (Fig. 2). Indeed, this convective line generated a F1 tornado at its south part about 25 min later (08:20 JST). Thick line in the figure indicates the direction of radial profiles of the data shown later, and the open circle on the line indicates the location of a Parsivel disdrometer at Sekiyado (SYD), 32 km apart from the radar.

a. Range profiles

Range profiles of raw- and smoothed-observed Φ_{DP} , and theoretical Φ_{DP} with and without attenuation correction for the 239° azimuth appear in Fig. 3. Another disdrometer located at the MRI site recorded a rainfall rate of 4 mm h^{-1} at the time, and a bias of 1.2 dB was added to compensate for the effect of wet radome to match $\Delta\Phi_{DP}$. The radial profiles of specific attenuation, A_H and specific differential attenuation, A_{DP} retrieved in the algorithm to calculate the attenuation-corrected-theoretical Φ_{DP} , appear in Fig. 4. Both A_H and A_{DP} were estimated from observed Z_H and Z_{DR} with the radar simulator. Both attenuations increase in the region where the gradient of Φ_{DP} ($= K_{DP}$) is large (Fig. 3). A profile of attenuation corrected Z_H can be derived from profiles of the observed Z_H and A_H (Fig 5). The discrepancy of the Z_H profiles becomes apparent beyond 25 km, where Φ_{DP} begins to increase with range (Fig. 3).

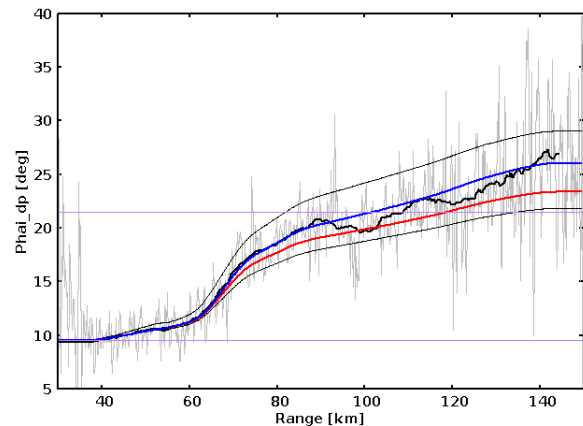


Fig. 1. Radial profiles of observed differential phase shift, Φ_{DP} (gray), observed differential phase shift smoothed along 66 (=10km) gates (black), theoretical differential phase shift without attenuation corrections (red), and with attenuation corrections (blue) for the 29° azimuth valid at 0253 JST 07 July 2010. Theoretical differential phase shifts with +1 and -1 dB perturbations in reflectivity are shown as thin black lines. Horizontal purple lines correspond to an initial differential phase value of 9.5° and final threshold value of 21.5° (initial + 12°).

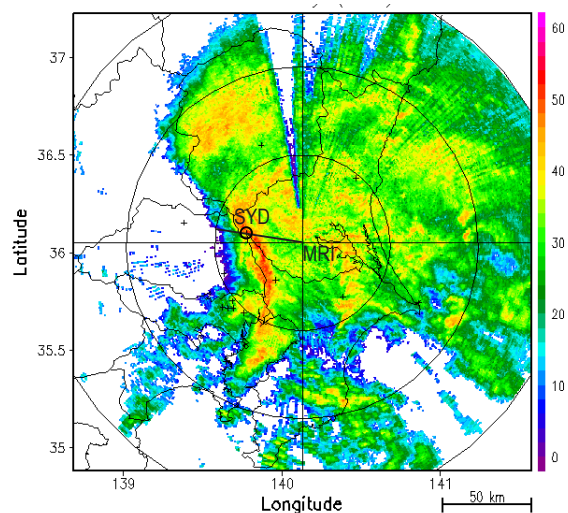


Fig. 2. Radar reflectivity field of the MRI C-band polarimetric radar at a 1.0° elevation angle at 07:54 JST on 3 December 2010. The color scale represents radar reflectivity in dBZ. Thick line in the figure depicts the direction of radial profiles analyzed in Figs. 3-6, and the open circle on the line indicates the location of the Parsivel disdrometer at Sekiyado (SYD), 32 km apart from the radar.

Range profiles of rainfall rates from the observed reflectivity and from the rain drop size distribution (DSD) estimated by the proposed algorithm are shown in Fig. 6. The red curve indicates the rainfall rate profile estimated from observed reflectivity by using the $R(Z_H)$ relationship (Hitschfeld and Bordan 1954). Again, the discrepancy of the two rainfall rate profiles becomes apparent around 25 km and takes maximum just behind 30 km in range where a disdrometer was located.

b. Comparison with disdrometer

To evaluate the reliability of the algorithm, we compared the estimated rainfall rate with that observed by a disdrometer (Parsivel) at Sekiyado, which was located 31.8 km west-northwest of the MRI site (Fig. 2). Time series of the rainfall rate derived from the Parsivel and the radar observations at Sekiyado is shown in Fig. 7. The radar-estimated rainfall rate data available for the single point nearest to the Sekiyado station was used for the comparison. The thick line shows the 1-min mean rainfall rate observed with the Parsivel, and the marks indicate the rainfall rate estimated every 2 minutes from DSD derived by the algorithm and an estimation from the $R(Z_H)$ relationship for reference. The figure clearly shows that the algorithm outperforms the $R(Z_H)$ relationship, particularly in heavy rainfall. The reliability of the algorithm is also confirmed by comparing estimated median volume diameter (D_0) with that measured with the disdrometer (Fig. 8) especially in heavy rain periods.

5. CONCLUSIONS

In this study we have demonstrated a calibration algorithm for C-band polarimetric radar. As an attenuation correction is included in the algorithm using polarimetric measurements, this method is immune to rain attenuation, and rainfall rate retrieved with this algorithm is expected to be highly reliable even in heavy rainfall. To evaluate the algorithm, we compared the rainfall rate and median volume diameter estimated by the algorithm with results obtained from an optical disdrometer on the ground. We demonstrated that the rainfall rate and D_0 estimated from this algorithm agreed well with the disdrometer results and was much more reliable than estimations derived from reflectivity alone. These results suggest that the calibration of Z_H measured with radars operating at C-band or higher frequency can be achieved much better than 1 dBZ with the proposed algorithm, and the rainfall rate retrieved by the algorithm is reliable even in heavy precipitation unless ice particles are included in the profile.

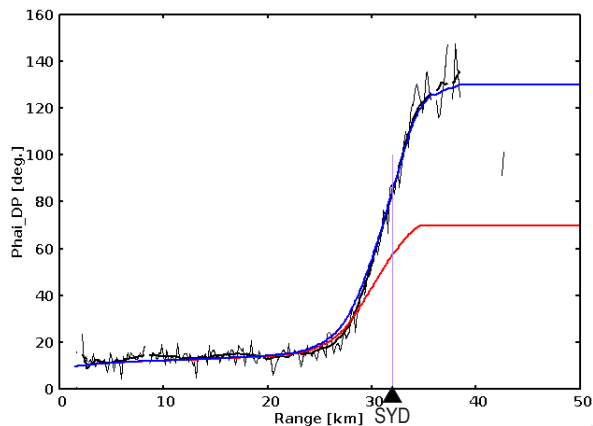


Fig. 3. Radial profiles of observed Φ_{DP} (thin-black), observed Φ_{DP} smoothed along 20 (=3 km) gates (thick-black), theoretical Φ_{DP} with attenuation corrections (blue), and without attenuation corrections (red) for the 239° azimuth at 07:54 JST on 3 December 2010. The purple vertical line indicates the location of a disdrometer at Sekiyado (SYD).

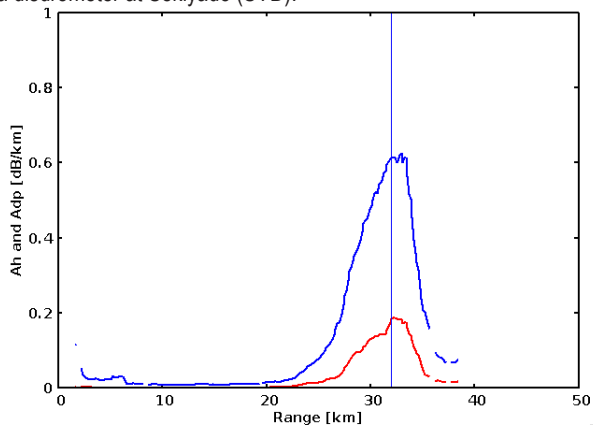


Fig. 4. Radial profiles of specific attenuation, A_H (blue), and specific differential attenuation, A_{DP} (red) estimated from polarimetric radar observations with a radar simulator for the 239° azimuth at 07:54 JST on 3 December 2010. The blue vertical line indicates the location of a disdrometer.

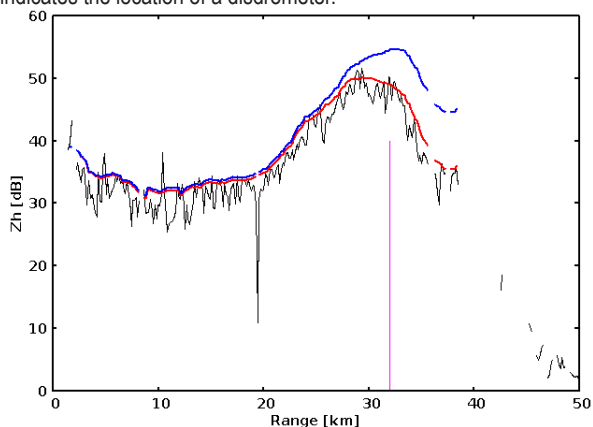


Fig. 5. Radial profiles of observed reflectivity factor, Z_H (black), observed reflectivity smoothed along radial (red), smoothed theoretical attenuation corrected reflectivity (blue) for the 239° azimuth at 07:54 JST on 3 December 2010. A bias of 1.2 dB due to the wet radome is added on the smoothed data. The purple vertical line indicates the location of a disdrometer.

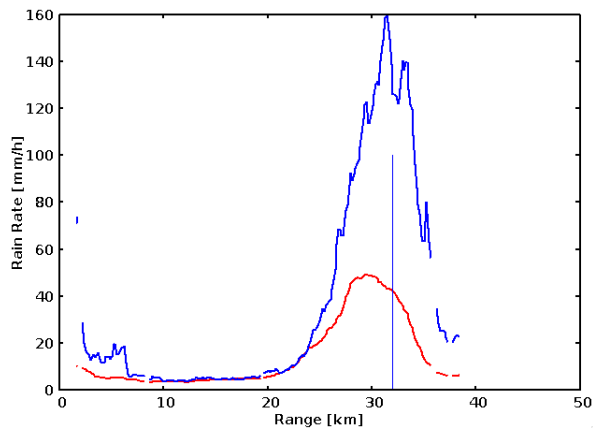


Fig. 6. Radial profiles of rainfall rate smoothed along 10 gates estimated from observed reflectivity (red) and from theoretical rain drop size distribution (blue) for the 239° azimuth at 07:54 JST on 3 December 2010. The blue vertical line indicates the location of the disdrometer.

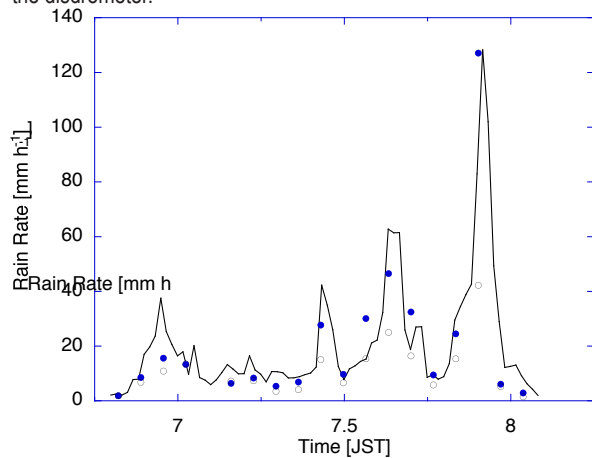


Figure 7. Rainfall rate comparisons between disdrometer measurements (solid line) and MRI C-band polarimetric radar estimations using the $R(DSD)$ method (closed circles) and from the observed reflectivity (open circles) at Sekiyado surface station from 06:45 to 08:15 JST.

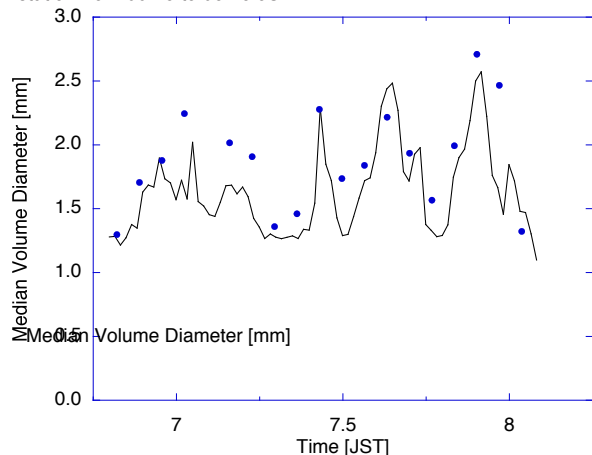


Fig. 8. Median volume diameter (D_0) comparisons between disdrometer measurements (solid line) and MRI C-band polarimetric radar estimations at Sekiyado surface station from 06:45 to 08:15 JST.

Acknowledgements

This study was partially supported by Japan Society for the Promotion of Science (JSPS) Grant-in-Aid for Scientific Research (22510200) and by the funds for integrated promotion of social system reform, research and development of the Ministry of Education, Culture, Sports, Science and Technology (MEXT) of Japan.

REFERENCES

- Adachi, A., T. Kobayashi, H. Yamauchi, and S. Onogi, 2013: Detection of potentially hazardous convective clouds with a dual-polarized C-band radar. *Atmos. Meas. Tech.* *accepted*.
- Anraku, N., M. Wada, A. Adachi, and H. Yamauchi, 2013: Solid-state pulse compression radars in Japan. *36th Conf. on Radar Meteorology*, Breckenridge, CO, Amer. Meteor. Soc., 158.
- Brandes, E. A., G. Zhang, and J. Vivekanandan, 2002: Experiments in rainfall estimation with a polarimetric radar in a subtropical environment. *J. Appl. Meteor.*, 41, 674-685.
- , 2005: Corrigendum. *J. Appl. Meteor.*, 44, 186-186.
- Bringi, V. N., and V. Chandrasekar, 2001: *Polarimetric Doppler Weather Radar: Principles and Applications*. Cambridge University Press.
- Bringi, V. N., and coauthors, 2006: Rainfall estimation from C-band polarimetric radar in Okinawa, Japan: Comparison with 2D-video disdrometer and 400 MHz wind profiler. *J. Meteor. Soc. Japan*, 84, 705-724.
- Goddard, J. W. F., J. Tan, and M. Thurai, 1994: Technique for calibration of meteorological radars using differential phase. *Electron. Lett.*, 30, 166-167.
- Gourley, J. J., A. J. Illingworth, and P. Tabary, 2009: Absolute calibration of radar reflectivity using redundancy of the polarization observations and implied constraints on drop shapes. *J. Atmos. Oceanic Technol.*, 26, 689-703.
- Hitschfeld, W., and J. Bordan, 1954: Errors inherent in the radar measurement of rainfall at attenuating wavelengths. *J. Meteor.*, 11, 58-67.
- Kobayashi, T., K. Masuda, H. Yamauchi, and A. Adachi, 2012: Physically-based simulator for measurements of precipitation with polarimetric and space-borne radars. *Remote Sensing of Clouds and the Atmosphere*, Prague, Czech Republic, SPIE, 8177, 817710-1 - 817710-6.
- Lhermitte, R., 1990: Attenuation and scattering of millimeter wavelength radiation by clouds and precipitation. *J. Atmos. Oceanic Technol.*, 7, 464-479.
- Thurai, M., W. A. Petersen, A. Tokay, C. Schultz, and P. Gatlin, 2011: Drop size distribution comparisons between Parsivel and 2-D video disdrometers. *Adv. Geosci.*, 30, 3-9.
- Tokay, A., W. A. Petersen, P. Gatlin, and M. Wingo, 2013: Comparison of raindrop size distribution measurements by collocated disdrometers. *J. Atmos. Oceanic Technol.*, 30, 1672-1690.
- Yamauchi, H., A. Adachi, O. Suzuki, and T. Kobayashi, 2012: Precipitation estimate of a heavy rain event using a C-band solid-state polarimetric radar. *7th European Conf. on Radar in Meteorology and Hydrology*.